Arabian Journal of Chemistry (2019) 12, 3652–3666

King Saud University

Arabian Journal of Chemistry

www.ksu.edu.sa
www.sciencedirect.com

ORIGINAL ARTICLE

Chemical characterization and cytotoxic potential of an ellagitannin-enriched fraction from *Fragaria vesca* leaves

Joana Liberal [a,b,c], Gustavo Costa [a,b,c], Anália Carmo [a,d], Rui Vitorino [e], Carla Marques [f], Maria Rosário Domingues [e], Pedro Domingues [e], Ana Cristina Gonçalves [a,g,h], Raquel Alves [a,g,h], Ana Bela Sarmento-Ribeiro [a,g,h,i], Henrique Girão [f], Maria Teresa Cruz [a,c,*], Maria Teresa Batista [a,b,c]

[a] *Center for Neurosciences and Cell Biology, University of Coimbra, Coimbra, Portugal*
[b] *Center for Pharmaceutical Studies, Faculty of Pharmacy, University of Coimbra, Coimbra, Portugal*
[c] *Faculty of Pharmacy, University of Coimbra, Coimbra, Portugal*
[d] *University School of Vasco da Gama, Coimbra, Portugal*
[e] *Mass Spectrometry Centre QOPNA, Department of Chemistry, University of Aveiro, Aveiro, Portugal*
[f] *Centre of Ophthalmology and Vision Sciences, Institute for Biomedical Imaging and Life Sciences (IBILI), Faculty of Medicine, University of Coimbra, Coimbra, Portugal*
[g] *Applied Molecular Biology and University Clinic of Hematology, Faculty of Medicine, University of Coimbra, Coimbra, Portugal*
[h] *Center of Investigation in Environment, Genetics and Oncobiology (CIMAGO), Faculty of Medicine, University of Coimbra, Coimbra, Portugal*
[i] *Clinical Hematology Department, Centro Hospitalar e Universitário de Coimbra (CHUC), Coimbra, Portugal*

Received 4 September 2015; accepted 21 November 2015
Available online 11 December 2015

KEYWORDS

Cancer;
HepG2;
Proteolytic pathways;
Proteome;
Cell proliferation;
Cell cycle

Abstract The hepatocellular carcinoma, a primary malignancy of the liver, has a very poor prognosis and a lower survival rate. Moreover, the inefficacy of conventional therapies emphasizes the importance of discovering new bioactive compounds. Several studies clearly state that plant-derived polyphenols, namely ellagitannins, have several health benefits. *Fragaria vesca* leaves contain high amounts of polyphenols, being especially rich in ellagitannins. Therefore, this study aimed to characterize an ellagitannin-enriched fraction (EEF) from *F. vesca* leaves and to unveil the anticancer potential of this fraction on human hepatocellular carcinoma cells.

Abbreviations: EEF, ellagitannin-enriched fraction

* Corresponding author at: Azinhaga de Santa Comba, 3000-548 Coimbra, Portugal. Tel.: +351 239 480209.
E-mail address: trosete@ff.uc.pt (M.T. Cruz).

Peer review under responsibility of King Saud University.

Production and hosting by Elsevier

http://dx.doi.org/10.1016/j.arabjc.2015.11.014
1878-5352 © 2015 The Authors. Published by Elsevier B.V. on behalf of King Saud University.
This is an open access article under the CC BY-NC-ND license (http://creativecommons.org/licenses/by-nc-nd/4.0/).

The analysis of EEF by HPLC-PDA-ESI/MS^n allowed the detection of 12 ellagitannins. The cell viability of both EEF and crude extract was determined after 24 h of cells treatment and the half-maximal inhibitory concentration (IC_{50}) was evaluated. The IC_{50} of the EEF (113 μg/mL) was about 6 times lower than the IC_{50} of the crude extract (690 μg/mL). Furthermore, EEF induced cell cycle arrest at G2/M checkpoint and decreased cell proliferation in a dose-dependent way. This fraction also induced an accumulation of LC3-II protein through blockage of autophagic flux, and inhibited chymotrypsin-like activity of 26S proteasome. These results showed, for the first time, that EEF from *F. vesca* leaves inhibits both, autophagic and ubiquitin-proteasome system pathways, two main intracellular protein degradation systems that are targets for anticancer therapies. Additionally, a proteomic analysis allowed the identification of 914 proteins, among which 133 were modulated after cells treatment with EEF, most of them related to metabolic pathways. Overall, this study shows that the EEF from *F. vesca* leaves decreased cell proliferation, inhibited the proteolytic mechanisms and modulated the metabolic pathways of the cell. Additionally this study points out *F. vesca* as a source of valuable molecules with anticancer potential, suggesting that ellagitannins, the polyphenols identified in this fraction, could be useful in the development of new fine-tuned therapeutic strategies against carcinogenesis.

© 2015 The Authors. Published by Elsevier B.V. on behalf of King Saud University. This is an open access article under the CC BY-NC-ND license (http://creativecommons.org/licenses/by-nc-nd/4.0/).

1. Introduction

Liver cancer is the sixth most frequent neoplasia and the third cause of cancer-related death worldwide (Center and Jemal, 2011). Hepatocellular carcinoma accounts for between 85% and 90% of primary liver cancers and generally occurs in patients with underlying chronic liver disease, especially with chronic hepatitis B virus (El-Serag and Rudolph, 2007). Hepatocellular carcinoma has a very poor prognosis because diagnosis is usually made at an advanced stage, when treatment options are limited and less effective (Lin et al., 2012). Therefore, the discovery of new bioactive molecules to overcome the inefficacy and the side effects of conventional therapies is still a hotspot of anticancer research.

Cancer cells are characterized by unbalanced control of cellular proliferation and an immortalized life span (Feitelson et al., 2015). Accordingly, any molecule capable of suppressing cancer cell proliferation may be valuable as a potential chemopreventive/chemotherapeu tic agent. Several polyphenols have shown the capacity to block the initiation of the carcinogenic process and to suppress both promotion and progression of cancer (Ramos, 2008). Apart from the well-known antioxidant properties of polyphenols, their role on cell growth (Kampa et al., 2007), apoptosis (Fresco et al., 2010) and cell proliferation (Giovannini and Masella, 2012) is also well established, being those effects usually cell type- and dose-dependent.

Ellagitannins (hydrolysable tannins) are bioactive polyphenols composed by moieties of hexahydroxydiphenoyl (HHDP) esterified to a sugar, usually the glucose, that release ellagic acid upon hydrolysis (Aguilera-Carbo et al., 2008). They are distributed in the plant kingdom (Okuda et al., 1993) and are commonly found in herbal preparations (Quideau, 2009), fruits (Aaby et al., 2007) and beverages (Lee and Talcott, 2002). Multiple biological activities have been ascribed to ellagitannins, namely antioxidant, anti-atherosclerotic, anti-inflammatory and anti-viral (Ascacio-Valdes et al., 2011). Furthermore, there is a wealth of information indicating the potent anticancer activities of ellagitannins (Auzanneau et al., 2012; Sartippour et al., 2008). Accordingly, some ellagitannins demonstrated to inhibit cell proliferation, which was in part due to their ability to arrest cell cycle (Cho et al., 2015; Vassallo et al., 2013). Additionally, these molecules have been shown to induce apoptotic cell death in different cell lines, modulating several molecular pathways and the expression of apoptotic regulators (Li et al., 2013; Wang et al., 2013).

Fragaria vesca L., commonly known as wild strawberry, is an herbaceous perennial plant that is primarily valued for their fruits, the strawberries. However, the leaf has a great pharmacological potential considering its traditional uses (Camejo-Rodrigues et al., 2003; Neves et al., 2009) and the presence of high amounts of bioactive compounds (Buricova et al., 2011; Ivanov et al., 2015). In fact, our group previously demonstrated that a crude extract obtained from *F. vesca* L. was enriched in polyphenols, namely ellagitannins, proanthocyanidins, and quercetin and kaempferol glucuronide derivatives, being ellagitannins the main phenolic compounds. In addition, we proved that this extract modulated the activity of the proteolytic mechanisms of the cells, the ubiquitin-proteasome system (UPS) and autophagy-lysosomal system (Liberal et al., 2014). These processes are responsible for the degradation of dysfunctional and damaged cellular components and their dysregulation is implicated in wide range of pathological conditions (Vilchez et al., 2014). Moreover, given their association with the carcinogenic process, these proteolytic pathways constitute privileged targets for anticancer therapies (Driscoll and Chowdhury, 2012).

In this study, we aimed to obtain an ellagitannin-enriched fraction (EEF) from the crude extract previously reported and to further explore the molecular mechanisms behind EEF bioactivity. Briefly, the polyphenols of this fraction were characterized and its cytotoxic effect on human hepatocellular carcinoma cells (HepG2) was evaluated. Then, we investigated the effect of EEF on cell proliferation, cell cycle and cell death, as well as its effect in the proteolytic mechanisms. Furthermore, a proteomic based approach was used to disclose differentially expressed proteins following cell treatment with this fraction, evaluating the main cellular processes modulated by EEF.

2. Material and methods

2.1. Materials

Fetal calf serum was obtained from GIBCO (Paisley, UK). Protease and phosphatase inhibitor cocktail tablets were acquired from Roche (Basel, Switzerland). Polyvinylidene fluoride (PVDF) membranes were obtained from Millipore Iberica (Madrid, Spain) and acrylamide from BioRad (Hercules, CA, USA). The following antibodies were used: anti-ubiquitin, clone P4D1 (Biolegend, San Diego, CA, USA), anti-microtubule-associated protein light chain 3 (LC3) (Cell Signaling Technologies, Danvers, MA, USA), anti-insulin-like growth factor-binding protein 1 (IGFBP1) (Abcam, Cambridge, UK), anti-fatty acid synthase (FAS) (Cell Signaling

Technologies, Danvers, MA, USA), and anti-β-tubulin antibody (Sigma Chemical Corporation, St. Louis, MO, USA). Enhanced chemifluorescence (ECF) substrate, anti-mouse and anti-rabbit alkaline phosphatase-conjugated secondary antibodies were purchased from GE Healthcare (Chalfont St. Giles, UK). Suc-Leu-Leu-Val-Tyr-AMC (Suc-LLVY-AMC) was from Enzo Life Sciences (Farmingdale, NY, USA). Click-iT® EdU Alexa Fluor® 488 Flow Cytometry Assay Kit was obtained from Molecular Probes, Invitrogen (Eugene, OR, USA) and propidium iodide (PI) with RNase solution and annexin V-fluorescein isothiocyanate (FITC)/PI from Immunostep (Salamanca, Spain). All other reagents were acquired from Sigma Chemical Corporation (St. Louis, MO, USA) and Merck (Darmstadt, Germany).

2.2. Plant material

F. vesca wild plants (with flowers and fruits) were sustainably collected from Granja de Figueira do Lorvão, Penacova, Portugal (May, 2011). A voucher specimen (ID-180611) was deposited at the Herbarium of Medicinal Plants, Faculty of Pharmacy, University of Coimbra.

The leaves were separated from stems, flowers and fruits and dried in a drying oven during 24 h, at 30 °C with forced air circulation. They were powdered and sieved before extraction.

2.3. Extract fractionation

A hydroalcoholic extract from *F. vesca* leaves was prepared as previously described (Liberal et al., 2014). Briefly the dry and powdered leaves were treated with dichloromethane (2 times) and the extraction was performed with ethanol (2 times) and 50% aqueous ethanol (3 times) at room temperature using an Ultra-Turrax homogenizer for 5 min at 8000–9500 rpm. The ethanol and hydroalcoholic extracts were combined and concentrated on a rotatory evaporator to a small volume and lyophilized. This extract was stored at −20 °C until the time for testing.

The lyophilized extract (3 g) was recovered with 50% aqueous methanol and fractionated by gel chromatography on a Sephadex® LH-20 (Sigma-Aldrich) column (25 cm × 5 cm) by elution successively with 50% (2 L) and 75% aqueous methanol (2.5 L) and 70% aqueous acetone (1 L).

All the fractionation process was monitored by high-performance liquid chromatography (HPLC) providing 8 major fractions: F1 (174 mL; phenolic acids), F2 (320 mL; phenolic acids and flavonoids;), F3 (710 mL; flavonoids), F4 (1198 mL; gallotannins and ellagic acid), F5 (704 mL; proanthocyanidins and ellagic acid), F6 (1087 mL; proanthocyanidins and ellagic acid), F7 (383 mL; proanthocyanidins) and F8 (946 mL; ellagitannins). The polyphenol-rich fractions were then taken to dryness under reduced pressure on a rotatory evaporator, at 40 °C, lyophilized and weighted in sterilized and humidity-controlled conditions.

Since ellagitannins were one of the main phenolic compounds of the hydroalcoholic extract, an EEF was selected to evaluate the effect of these polyphenols in the hepatocellular carcinoma cell line. Ellagitannins were only identified in this fraction, which was obtained with 70% aqueous acetone (yield of 14% of 100 g of the *F. vesca* extract). The yields of the remaining fractions were the following: F1 – 48%, F2 – 19%, F3 – 8%, F4 – 3%, F5 – 3%, F6 – 3% and F7 – 1%.

2.4. HPLC-PDA-ESI/MS^n analysis

Polyphenols structural identification of EEF was carried out on a Surveyor liquid chromatograph equipped with a PDA detector (Surveyor) and interfaced with a Finnigan LCQ Advantage Ion Max MS^n mass spectrometer (Thermo Fisher Scientific) equipped with an API-ES ionization chamber. Separation occurred on a Spherisorb ODS-2 column (150 × 2.1 mm i.d.; particle size, 3 μm; Waters Corp.) and a Spherisorb ODS-2 guard cartridge (10 × 4.6 mm i.d.; particle size, 5 μm; Waters Corp.) at 25 °C, using 2% aqueous formic acid (v/v) (A) and methanol (B) as mobile phase. The gradient profile was 5–15% B (0–10 min), 15–25% B (10–15 min), 25–50% B (15–50 min), 50–80% B (50–60 min), 80–100% B (60–70 min) and an isocratic elution for 5 min, at a flow rate of 200 μL min^{-1}. The first detection was performed on PDA detector in a wavelength range 200–450 nm, followed by a second detection in the mass spectrometer. Mass spectra were acquired in negative ion mode. The mass spectrometer was programmed to perform four consecutive scans: full mass (m/z 125–2000), MS^2 of the most abundant ion in the full mass, MS^3 of the most abundant ion in the MS^2 and MS^4 of the most abundant ion in the MS^3. Source voltage was 4.7 kV and the capillary voltage and temperature were −7 V and 275 °C, respectively. Nitrogen was used as sheath and auxiliary gas at 20 and 7 Finnigan arbitrary units, respectively. The normalized energy of collision was 49%, using helium as collision gas. Data treatment was carried out with XCALIBUR software (Thermo Scientific).

2.5. Cell culture

Human hepatic carcinoma cell line (HepG2 – ATCC HB-8065) was kindly supplied by Professor Conceição Pedroso Lima (Center for Neurosciences and Cell Biology, University of Coimbra, Portugal) and cultured in Dulbecco's Modified Eagle Medium (DMEM) containing 10% (v/v) heat-inactivated fetal bovine serum, 100 U/mL penicillin, and 100 μg/mL streptomycin. Cells were maintained at 37 °C and 5% CO_2 in a humidified incubator.

2.6. Assessment of cell viability

The effect of EEF on cell viability/metabolic activity was evaluated by resazurin assay (O'Brien et al., 2000). Cells (8×10^4 cells/well) were plated in 96-well plates, in duplicates, for 12 h and incubated with serial concentrations of EEF for 24 h. Resazurin (50 μM) was added to the cells 1 h before recording fluorescence. Absorbance was recorder at 570 nm, with a reference wavelength of 620 nm, using a standard spectrophotometer (SLT, Austria). In this assay, metabolic active cells reduce resazurin (blue dye) into resorufin (pink colored); therefore, their number correlates with the magnitude of dye reduction. Cell viability was evaluated based on a comparison with untreated cells. The half-maximal inhibitory concentration (IC_{50}) represents the EEF concentration required to inhibit 50% of cell viability and was determined by nonlinear regression.

2.7. Cell proliferation, cell cycle and cell death analysis

Cells (6.4×10^5) were plated in 12-well plates. HepG2 proliferation was assessed by incorporation of 5-ethynyl-2′-deoxyuridine (EdU), a thymidine analog that is incorporated into DNA of dividing cells during S phase. Cells were treated with different concentrations of EEF for 24 h and EdU (10 μM) was added 3 h before cell fixation with 70% aqueous ethanol. Click-iT® EdU Alexa Fluor® 488 Flow Cytometry Assay Kit was performed according to the manufacturer's instructions (Molecular Probes, Invitrogen).

Cell cycle distribution was analyzed after 24 and 48 h of EEF addition. Cells were harvested by trypsinization, washed twice and fixed with 70% ice-cold aqueous ethanol overnight and then incubated with PI with RNase solution for 15 min at room temperature before analysis.

After cells incubation for 24 h with EEF, apoptosis was detected using an annexin V-fluorescein isothiocyanate (FITC)/PI double staining, as described by the supplier (Immunostep).

All the flow cytometry measurements were performed on a Becton Dickinson FACSCalibur cytometer using the Cellquest software (BD Biosciences). PI histogram modeling was performed in ModFit LT software (Verity Software House). The flow cytometer was calibrated with fluorescent standard microbeads (CaliBRITE Beads; BD Biosciences) for accurate instrument setting.

2.8. Morphological analysis with May-Grünwald-Giemsa and Hoechst 33258

After 24 h of EEF treatment cells were trypsinized, resuspended in 30 μl of FBS and placed on a slide for microscopic analysis. The cells were stained for 3 min with May-Grünwald solution (0.3% v/v in methanol, then diluted in distilled water at 1:1 (v/v) ratio) and finally incubated during 15 min with Giemsa solution (0.75% w/v in glycerol/methanol 1:1) previously diluted in distilled water (8×). Cells were rinsed with distilled water and then left to dry at room temperature. Cell morphology was analyzed by light microscopy using an Olympus BX51TF microscope (Olympus Co. Ltd.)

For nuclear Hoechst-33258 staining cells were plated in 8-well chambered slides. After 24 h of treatment with EEF, cells were washed with PBS and fixed with 4% paraformaldehyde for 10 min, washed with PBS and incubated with 5 μg/mL Hoechst 33258 for 5 min at room temperature. Nuclear morphology was visualized under a fluorescence microscope (Leica DM4000B, Leica Microsystems).

2.9. Western blot analysis

Protein samples preparation, quantification and western blot were performed as previously described (Liberal et al., 2014). The antibodies were used in the following concentrations: anti-ubiquitin, clone P4D1 (1:2000), anti-LC3 (1:1000), anti-IGFBP1 (1:1000), anti-FAS (1:1000), anti-β-tubulin (1:20,000), and anti-mouse and anti-rabbit alkaline phosphatase-conjugated secondary antibodies (1:20,000).

2.10. Proteasome chymotrypsin-like activity

HepG2 cells were lysed in 50 mM Tris–HCl buffer (pH 7.6) containing 1 mM dithiothreitol and 2 mM of adenosine triphosphate (ATP). Equal amounts of protein were incubated with the proteasome substrate (fluorogenic) Suc-Leu-Leu-Val-Tyr-AMC (Suc-LLVY-AMC). Enzymatic kinetic was measured, during 30 min, in a temperature-controlled microplate fluorometric reader (37 °C), with excitation/emission wavelengths of 380/440 nm. The proteasome inhibitor MG132 was used as a positive control for proteasome activity inhibition.

2.11. Isobaric tag for relative and absolute quantitation (iTRAQ)-based proteomics labeling

Cells were plated, allowed to stabilize for 12 h and incubated with EEF concentration corresponding to IC_{50} (113 μg/mL) for 24 h. Cells were harvested and resuspended in HEPES-EDTA buffer (50 mM HEPES, 1 mM EDTA, pH 7.4). Then, the samples were sonicated (3 times for 5 s at 30 μm peak to peak) in a Vibra Cell sonicator (Sonics & Materials, Inc.) and centrifuged at 14,000 rpm for 10 min at 4 °C to remove cell debris. The supernatant was collected and protein concentration was assessed by bicinchoninic acid assay. For iTRAQ-based quantitative proteomic analysis, 100 μg of protein of each sample was prepared. The proteins were precipitated with 6 volumes of cold acetone at −20 °C overnight and centrifuged for 30 min at 14,000 g. Then, pellets were resuspended with triethylammonium bicarbonate buffer (TEAB) (0.1 M, pH 8.5) and 2% SDS to achieve a final concentration of 0.05%. Samples were then reduced with 50 mM tris (2-carboxyethyl) phosphine (TCEP) for 1 h at 37 °C. Following this, samples were alkylated with 10 mM S-methyl methanethiosulfonate (MMTS) (Sigma-Aldrich) for 10 min at room temperature with agitation. Trypsin was added to each sample and the digestion was performed for 18 h at 37 °C. Digested sample peptides were subsequently labeled with the iTRAQ® reagent – 8plex (ABSciex) following the protocol provided by the manufacturer. Labels were reconstituted in 60% isopropanol, added to each sample peptides and incubated for 2 h at room temperature with agitation. The reaction was stopped by adding water and acidified with formic acid (0.1% final concentration). Labeled samples were then combined and dried in SpeedVac.

Labeled peptides were separated from an adapted multidimensional liquid chromatography approach, as described by Vitorino et al. (2012) based on high pH for the first dimension peptide chromatography with a C18 reverse phase HPLC column and acidic pH for the second one. Thus, sample loading was performed at 200 μL/min with buffers (A) 2% ammonium hydroxide and 0.014% formic acid in water, pH 10 and (B) 2% ammonium hydroxide and 90% acetonitrile (ACN) in water, pH 10. After 5 min of sample loading and washing, peptide fractionation was performed with linear gradient to 70% B over 85 min. Sixty fractions were collected, dried in a SpeedVac and resuspended in 5% ACN and 0.1% trifluoroacetic acid (TFA). Collected fractions were then separated by LC. Peptides were loaded onto a C18 pre-column (5 mm particle size, 5 mm; Dionex) connected to an RP column PepMap100 C18 (150 mm_75 mm i.d., 3 mm particle size). The flow-rate was set at

300 nl/min. The mobile phases A and B were 2% ACN and 0.05% TFA in water, and 90% ACN with 0.045% TFA in water, respectively. The gradient started at 10 min and ramped to 60% B till 50 min and 100% B at 55 min and retained at 100% B till 65 min. The separation was monitored at 214 nm using a UV detector (Dionex/LC Packings). Using the micro-collector Probot (Dionex/LC Packings) and, after a lag time of 15 min, peptides eluting from the capillary column were mixed with a continuous flow of alpha-CHCA matrix solution (in internal standard Glu-Fib) and were directly deposited onto the LC-MALDI plates. The spectra were generated and processed with 4800 MALDI-TOF/TOF. Protein identification based on MS/MS data was performed with ProteinPilot™ software (v.4.0, ABSciex) using Paragon search method. SwissProt from *homo sapiens* (release date 06022013) was used as protein database. Default search parameters used were as follows: trypsin as the digestion enzyme, carbamidomethyl modification on cysteine residue and iTRAQ 8-plex. Bias correction was applied and proteins were identified with a confidence level of 95%. Proteins were found to be differentially expressed when $p < 0.05$ (FDR-corrected).

2.12. Statistical analysis

The results are expressed as mean ± standard error of the mean (SEM). Data were analyzed using one-way analysis of variance (ANOVA), followed by *Dunnett's post-hoc test*. The differences between the means were considered significant for values of $p < 0.05$. The statistical analysis was performed using Prism 5.0 Software (GraphPad Software).

3. Results and discussion

3.1. Phytochemical characterization of EEF

HPLC-PDA phenolic profile was recorded at 280 nm (Fig. 1) and 12 compounds were tentatively identified by HPLC-PDA-ESI/MS^n as ellagitannins (Table 1), based on their characteristic UV and MS spectra. All these compounds exhibit a characteristic UV spectrum with maximum absorbance below 270 nm such as those referred by Arapitsas (2012). Almost all compounds presented a maximum at 248–257 nm with a slight shoulder between 280 and 284 nm, a characteristic UV spectral profile that has been referred as a slope (Hanhineva et al., 2008).

Particular fragmentation patterns are described as follows: Peak **1** showed a $[M-H]^-$ ion at *m/z* 965 and the fragmentation originated a third order ion that matches with ellagic acid (*m/z* 301). Hanhineva et al. (2008) found similar molecules on stamens of *Fragaria ananassa* flowers, however the ellagitannin structure was not elucidated yet (Supplementary Fig. 1).

Peaks **2** and **6** were identified as sanguiin H-10 isomers. Peak **2** presented a $[M-2H]^{2-}$ at *m/z 783* and peak **6** evidenced a $[M-H]^-$ ion at *m/z* 1567, *giving a molecular mass of 1568*. The fragmentation patterns were slightly different. Peak **2** originated a most intense MS^2 ion at *m/z* 633 (corresponding to one galloyl-HHDP-glucose unit) and MS^3 ion at *m/z* 301 (loss of galloyl-glucose residue), whereas peak **6** displayed a main MS^2 ion at *m/z* 1265 (loss of HHDP unit), MS^3 ion at *m/z* 935 (loss of galloyl-glucose residue), and MS^4 ions at *m/z* 633 (loss of other HHDP unit) and 301 (HHDP unit, corresponding to a loss of HHDP-galloyl-glucose) (Mullen et al., 2003).

Peaks **3** and **5** evidenced a $[M-H]^-$ ion at *m/z* 933, MS^2 fragments at *m/z* 451 from the cleavage of tri-galloyl unit and spontaneous lactonization, 631 from the loss of HHDP unit and 301 which corresponds to ellagic acid residue. These compounds were tentatively identified as isomers of vescalagin/castalagin (Simirgiotis and Schmeda-Hirschmann, 2010).

Peaks **4** and **7** were identified, according to Kool et al. (2010), as sanguiin H-2 and presented a mono charged molecular ion at *m/z* 1103. The fragmentation pattern of peaks **4** and **7** was similar in MS^2, however the most intense fragments dif-

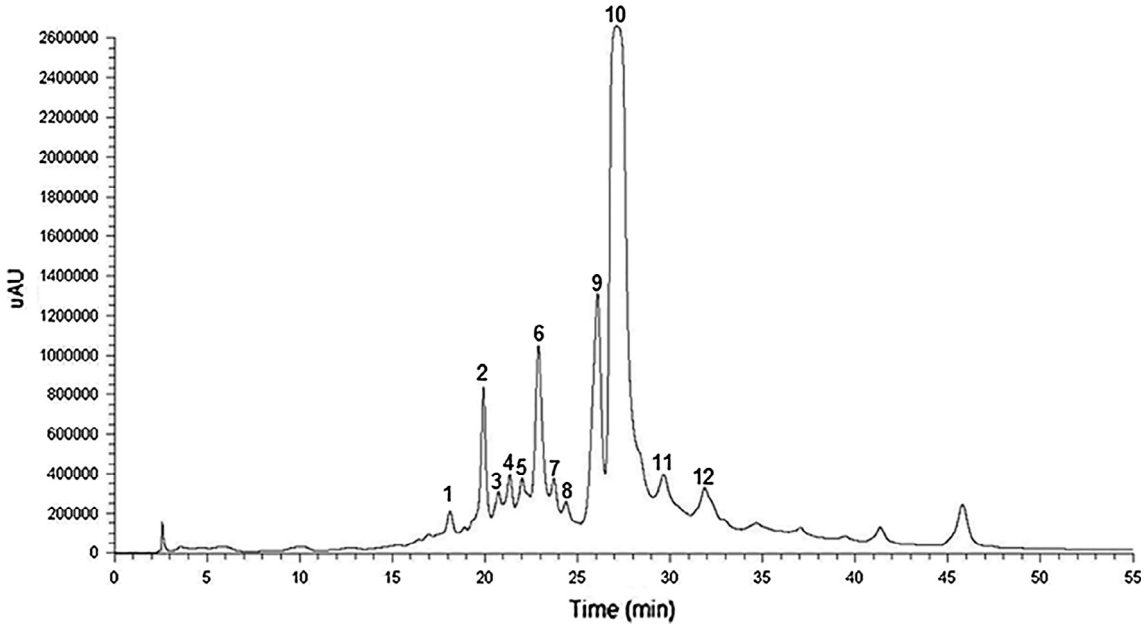

Figure 1 HPLC polyphenolic profile of EEF recorded at 280 nm. The identification of the peaks is shown in Table 1.

Table 1 Structural elucidation of ellagitannins of an enriched fraction obtained from *Fragaria vesca* leaves.

Peak	*Rt* (min)	λ_{max} (nm)	MW	$[M-H]^-$ (*m/z*)	MS^2	MS^3	MS^4	Compound tentatively identified
					m/z[a]			
1	18.12	250, 282sh	966	965	**783**	481, **301**, 275	–	Unknown ellagitannin
2	19.92	255, 283sh	1568	783[b]	1265, 935, 915, 897, **633**, 613, 301	**301**	–	Sanguiin H-10 isomer
3	20.75	250, 283sh	934	933	631, **451**, 301	433, 407, **405**, 327, 283	–	Castalagin/vescalagin isomer
4	21.35	251, 283sh	1104	1103	1059, **935**, 915, 897, 782	**633**, 301	**301**	Sanguiin H-2 isomer
5	21.97	250, 283sh	934	933	631, **451**	434, 407, **405**, 351, 301, 283	348, **377**	Castalagin/Vescalagin isomer
6	22.89	257, 282sh	1568	1567	**1265**, 963, 935, 915, 897, 783, 633, 613	1097, 963, **935**, 897, 783, 613	633, **301**	Sanguiin H-10 isomer
7	23.72	250, 282sh	1104	1103	**1059**, 935, 757	**935**, 897, 757, 633, 613	898, 877, **633**	Sanguiin H-2 isomer
8	24.37	248, 282sh	936	935	**633**, 301	463, **301**	–	Casuarictin/Potentillin isomer
9	26.07	257, 282sh	936	935	**633**, 301	463, **301**	–	Casuarictin/Potentillin isomer
10	27.12	258, 284sh	1870	1869	1567, 1265, 1085, **935**, 963, 897, 633	898, **633**, 465, 301	**301**, 275	Sanguiin H-6/Agrimoniin/ Lambertianin A isomer
11	29.64	252, 280sh, 370	1118	1117	**935**, 897, 633	**633**, 301	481, **301**	Unknown ellagitannin
12	31.87	250, 284sh	2020	1009[b]	1717, 1567, 1235, **1085**, 1065, 935, 897, 783, 451	**897**	–	Unknown ellagitannin

[a] The most abundant ions are shown in bold.
[b] Doubly charged ion $[M-2H]^{2-}$.

fered, showing a fragment at *m/z* 935 (−44 and −124 amu, a loss of CO_2 and trihydroxybenzene) and 1059 (−44 amu, a loss of CO_2), respectively. In MS^3, the parent MS^2 ion at m/z 935 (peak **4**) produced ions at *m/z* 633 (−302 amu, a loss of HHDP) and 301 (−302 and −332 amu, a loss of HHDP and of galloyl-glucosyl moieties respectively), while the parent MS^2 ion of peak **7**, at *m/z* 1059, gave a main fragment at *m/z* 935 (−124 amu, loss of trihydroxybenzene) and the ions at 897 (−162 amu, a loss of glucosyl moiety) and 633 (−44, −124 and −302 amu, a loss of CO_2, trihydroxybenzene and HHDP moieties).

Peaks **8** and **9** were identified as the isomeric forms of casuarictin or potentillin and presented a molecular ion at *m/z* 935 and MS^2 main fragments at *m/z* 633 (−302 amu) corresponding to one galloyl-HHDP-glucose unit and the ion at *m/z* 301 originated from lactonization of fragment 302 (Hanhineva et al., 2008). In the MS^3 the fragments at *m/z* 463 and 301 suggest the successive loss of the galloyl and galloylglucose residues.

Peak **10** is the major compound of this fraction and was also the main component of the crude extract. It showed a $[M-H]^-$ ion at *m/z* 1869 and MS^2 ions at *m/z* 1567 (loss of an HHDP unit), 1265 (loss of bis-HHDP), 1085 (loss of bis-HHDP-glucose) and 935, the main fragment, corresponding to one galloyl-bis-glucose unit. This fragmentation matched with sanguiin H-6/agrimoniin/lambertianin A isomers, previously identified in the leaves of *Fragaria* species (Simirgiotis and Schmeda-Hirschmann, 2010). The third and fourth orders of fragmentation pattern confirmed the identification as evidenced, respectively by ions at *m/z* 633 (935 − 302 amu, loss of HHDP unit) and 301 (633 − 332, loss of galloyl-glucose residue).

Peak **11** displayed a $[M-H]^-$ ion at *m/z* 1117, giving a molecular mass of 1118. The structure of this molecule was not fully elucidated. However, the fragmentation pattern is consistent with an ellagitannin as evidenced by the main MS^2 ion at *m/z* 935 (corresponding to a galloyl-bis-HHDP-glucose), MS^3 ion at *m/z* 633 (loss of HHDP) and MS^4 at *m/z* 301 (loss of galloyl-glucose residue) (Supplementary Fig. 2).

Peak **12** presented a $[M-2H]^{2-}$ at *m/z* 1009, giving a molecular mass of 2020 Da, and MS^2 fragments at *m/z* 1717, 1567, *1235,* 1085, 1065, 935, 897, 783 and 451 (Supplementary Fig. 3). An ellagitannin with the same molecular mass and a similar fragmentation pattern was also previously reported in *Fragaria* spp (Gasperotti et al., 2013).

Several ellagitannins identified in the EEF were also previously disclosed in strawberries (Gasperotti et al., 2013; Simirgiotis and Schmeda-Hirschmann, 2010; Vrhovsek et al., 2012) – fruits well-known for their anticarcinogenic, antioxidant and genoprotective properties (reviewed in Giampieri et al., 2012). The major peak of the fraction, identified as sanguiin H-6, agrimoniin or lambertianin A isomer, was also the major compound of the crude extract. Although there are still few studies with the isolated molecules, the anticancer activities of these proposed compounds were previously addressed in other cells. For example, it was demonstrated that agrimoniin induces apoptosis in human gastric cancer cells (SGC-7901) (Wang and Jin, 2011) and sanguiin-H6 isolated from blackberry seeds extracts protects the DNA of human lymphocytes (Gođevac et al., 2011). These results suggest the importance of the ellagitannins as anticancer natural molecules.

3.2. Effect of F. vesca leaves crude extract and EEF on cell viability

Once identified the compounds present in the EEF we proceeded to evaluate the biologic effects of this fraction on HepG2 cells. We started to determinate the IC_{50} for cell viability of both, the EEF and the crude extract of *F. vesca* leaves. Resazurin reduction colorimetric assay was used to assess the cell viability after 24 h of treatment with increasing concentrations of the extract and fraction (up to 10,000 μg/mL). In order to determine cell sensitivity to treatments, data points of the dose-response curves were fitted with a sigmoid function for the calculation of the IC_{50} values. Data showed that both treatments reduce cell viability in a dose-dependent manner as represented in Fig. 2A. In fact, the IC_{50} of EEF was 6 times lower (113 ± 1 μg/mL) than the IC_{50} of the crude extract (690 ± 1 μg/mL), suggesting that ellagitannins could be responsible for the cytostatic/cytotoxic effect of the extract. Based on the high effect of the fraction relatively to the extract, all the subsequent experiments were performed only with EEF. Since ellagitannins yield ellagic acid on neutral and alkaline conditions (Daniel et al., 1991; Ross et al., 2007) it would be conceivable that ellagitannins hydrolysis could occur in the culture medium, thus generating ellagic acid that could be responsible for the antiproliferative effect of EEF. However, the absence of any effect on cell viability after cells treatment with concentrations up to 250 μg/mL of ellagic acid (data not shown) led us to suggest that cytotoxic effects could be ascribed to ellagitannins.

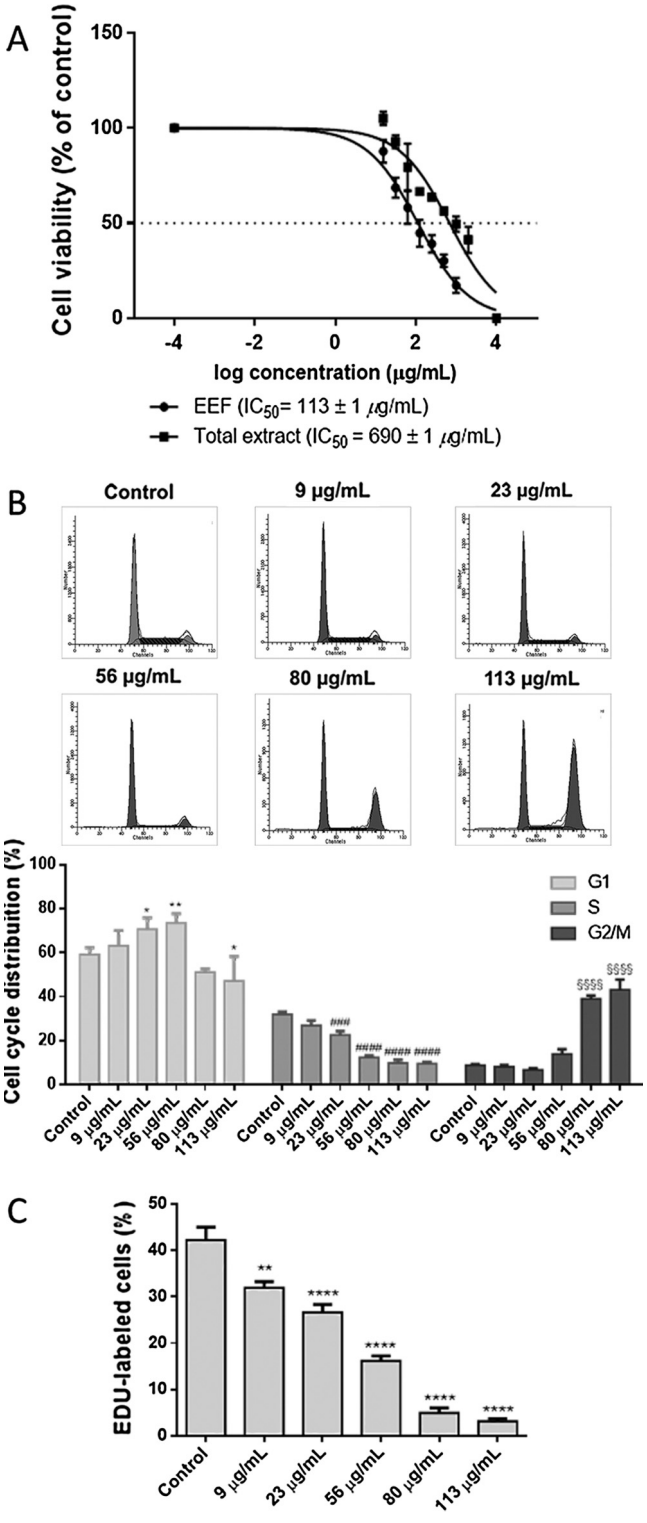

3.3. Cell cycle and cell proliferation after treatment with EEF

Defects in cell cycle checkpoints are associated with an uncontrolled cellular proliferation and, as such, targeting cell cycle could be an important strategy for cancer therapy. To further investigate alterations in the cell cycle of HepG2 cells exposed to EEF we used flow cytometry.

Cells were incubated with different concentrations of EEF during 24 h (IC_{50} = 113 μg/mL; IC_{45} = 80 μg/mL; IC_{40} = 56 μg/mL; IC_{25} = 23 μg/mL; IC_{15} = 9 μg/mL) and subsequently analyzed for the distribution of G0/G1, S and G2/M phases. EEF was able to interfere with cell cycle distribution, being the effect dependent on the concentrations used. In fact, higher concentrations of the EEF clearly induced an increase in cells in the G2/M phase whereas lower doses promoted a significant increase in cells in G1 when compared to control cells (Fig. 2B). Since tumor cells commonly adapt to toxic insults and recover over time we further evaluated whether EEF effects are sustained over time. For that, cells were treated with the same

Figure 2 Effect of EEF on HepG2 viability, cell cycle and cell proliferation. (A) Evaluation of cell viability after incubation with different concentrations of the extract or EEF for 24 h. Datapoints correspond to the mean ± standard deviation of at least three independent assays performed in duplicate. The IC_{50} values were fitted to a sigmoidal function from the dose-response curves. (B) Cell cycle distribution of cells treated with different concentrations of EEF for 24 h. Data are expressed as percentage of PI-positive cells and are given as the means ± SEM of at least three independent experiments. (C) EDU incorporation after the treatment with different concentrations of EEF. Data represent the mean ± SEM percentage of EDU-labeled cells from three independent experiments ($^{*}p < 0.05$, $^{**}p < 0.01$, $^{***}p < 0.001$, $^{****}p < 0.0001$ when compared to control; the symbols *, #, $, * were used for G1, S, G2/M and EDU, respectively).

concentrations of EEF for 48 h and a markedly G2/M cell cycle arrest was disclosed for the three higher concentrations tested (Supplementary Fig. 4). We may therefore point out that the inhibition of cell proliferation by EEF occurs, at least in part, through cell cycle arrest in G2/M phases.

We further evaluated HepG2 cell proliferation by the incorporation of EDU, determined by flow cytometry, after 24 h of EEF treatment. The results presented in Fig. 2C show that the incorporation of EDU is decreased for all the concentrations studied in a dose-dependent way, thus confirming and supporting the previous described effects on cell cycle.

As far as we know, the effect of the ellagitannins herein tentatively identified on cell cycle was never addressed. However, others ellagitannins were reported to modulate cell cycle distribution and cell cycle regulators, such as casuarinin (Kuo et al., 2005a, 2005b) and geraniin (Vassallo et al., 2013).

3.4. Apoptosis/Necrosis detection in EEF-treated cells

In order to evaluate cell death and to discriminate between apoptosis and necrosis triggered by the EEF treatment, cells were incubated with different concentrations of EEF for 24 h and then stained with annexin V-FITC/PI. The two higher concentrations of EEF promoted an increase in necrotic cells (annexin V-negative/PI-positive cells). This increase was accompanied by a rise, although not statistically significant, of annexin V-positive/PI-positive cells that correspond to late apoptotic/necrotic cells (Fig. 3A). To further clarify the mechanism of cell death, changes in cell morphology were evaluated through May-Grunwald-Giemsa staining. Cells treated with EEF for 24 h showed both features of necrosis (swelling, loss of membrane integrity) and apoptosis (membrane bleeding and cell shrinkage), with a predominance of a necrotic cell

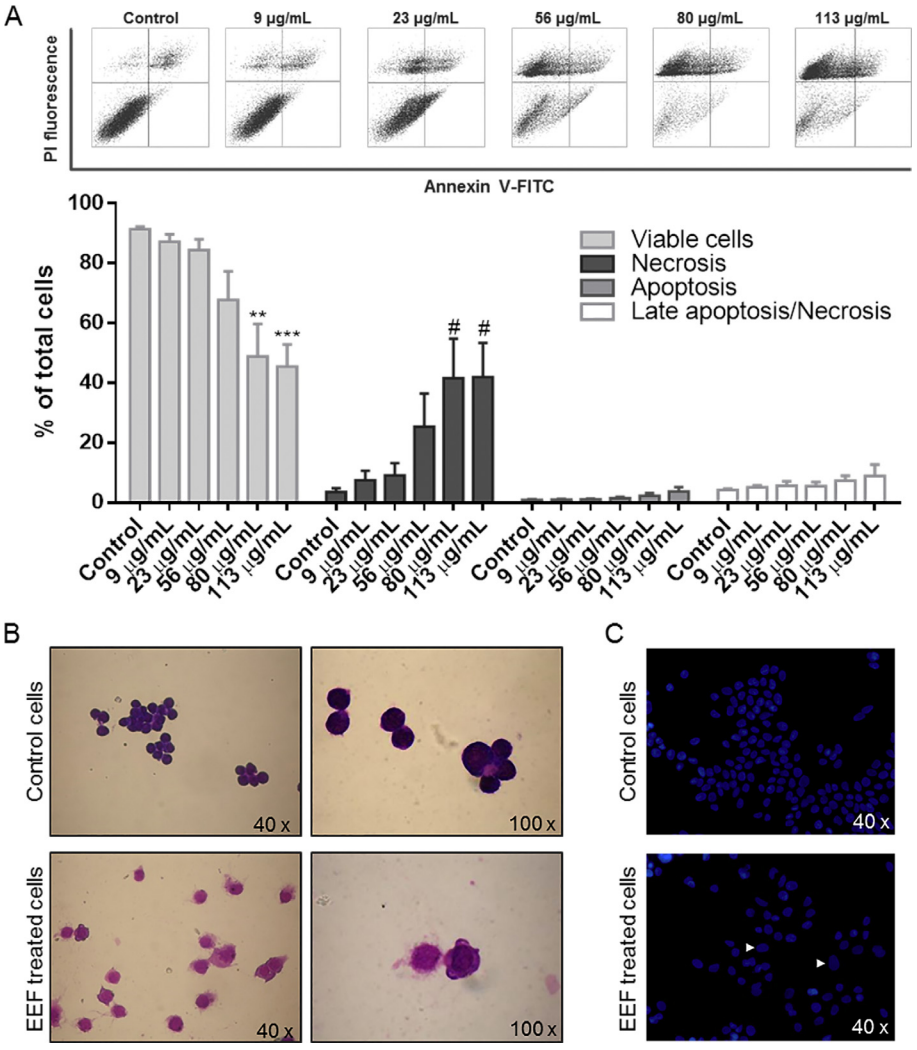

Figure 3 Detection of apoptosis/necrosis after EEF treatment. Cells were incubated with different concentrations of EEF for 24 h. (A) Annexin V-FITC/PI labeling was detected by FACSCalibur flow cytometer. The populations of early apoptotic cells (annexin V-positive/PI negative), late apoptotic cells (annexin V positive/PI positive), necrotic cells (annexin V negative/PI positive) and viable cells (annexin V negative/PI negative) were evaluated as a percentage of total cells and are given as the means ± SEM of at least three independent experiments ($^{*}p < 0.05$, $^{**}p < 0.01$, $^{***}p < 0.001$ when compared to control; the symbols * and # were used for viable and necrotic cells respectively). (B) Evaluation of morphology of cells stained with May-Grunwald-Giemsa and observed under light microscopy. Cells were visualized at 40× and 100× magnification. (C) Evaluation of nuclear morphology of cells stained with Hoechst 33258 and visualized under fluorescent microscopy at 40× magnification. Arrowheads show nuclear swelling.

death (Fig. 3B). Furthermore, nuclear morphology of HepG2 cells was assessed with Hoechst 33258. The results indicated that most of the nuclei are similar to those of control. Nevertheless, larger nuclei that could be related to necrotic cell death were occasionally observed (Fig. 3C).

Previous studies indicated that ellagitannins induce apoptotic cell death in *in vitro* and *in vivo* models (Wang et al., 2014; Li et al., 2013). Therefore, it was expected that cells end up dying by apoptosis. However, we did not detect an increase in apoptotic cells, neither through the analysis with PI, nor with annexin V/PI experiment and although the May-Grunwald-Giemsa staining allowed the visualization of apoptotic cells, necrosis was clearly the predominant mechanism of cell death. Accordingly, several studies demonstrated that the induction of apoptotic cell death evoked by ellagitannins was accompanied by an increase of necrosis (Cho et al., 2015; Kasimsetty et al., 2010). Importantly, while initially described as a nonregulated mechanism of death, necrosis is currently considered a consequence of the crosstalk between several biochemical and molecular events (Festjens et al., 2006). Necrosis occurs in both physiological and pathophysiological processes and in contrast to apoptosis, typically promotes an inflammatory response, which may contribute for the tumor regression. On the other hand, during tumor development, the inflammation due to the excessive spontaneous necrosis may stimulate the growth and aggressiveness of the tumor (Proskuryakov and Gabai, 2010).

3.5. EEF effect on the cellular proteolytic mechanisms

Our previous data established that *F. vesca* leaves crude extract modulates chymotrypsin-like activity of proteasome and autophagy (Liberal et al., 2014). Consequently, in this work we sought to evaluate whether the EEF displays similar bioactivity.

Cells were treated with different concentrations of EEF and the proteasome inhibitor MG132 was used as control. EEF significantly decreased chymotrypsin-like activity of the 26S proteasome after 6 and 24 h of treatment in a dose-dependent way (Fig. 4A and B, respectively). A decrease in proteasome degradation would lead to an accumulation of polyubiquitinated proteins. Accordingly, for the highest EEF concentrations tested during 24 h, an accumulation of ubiquitinated

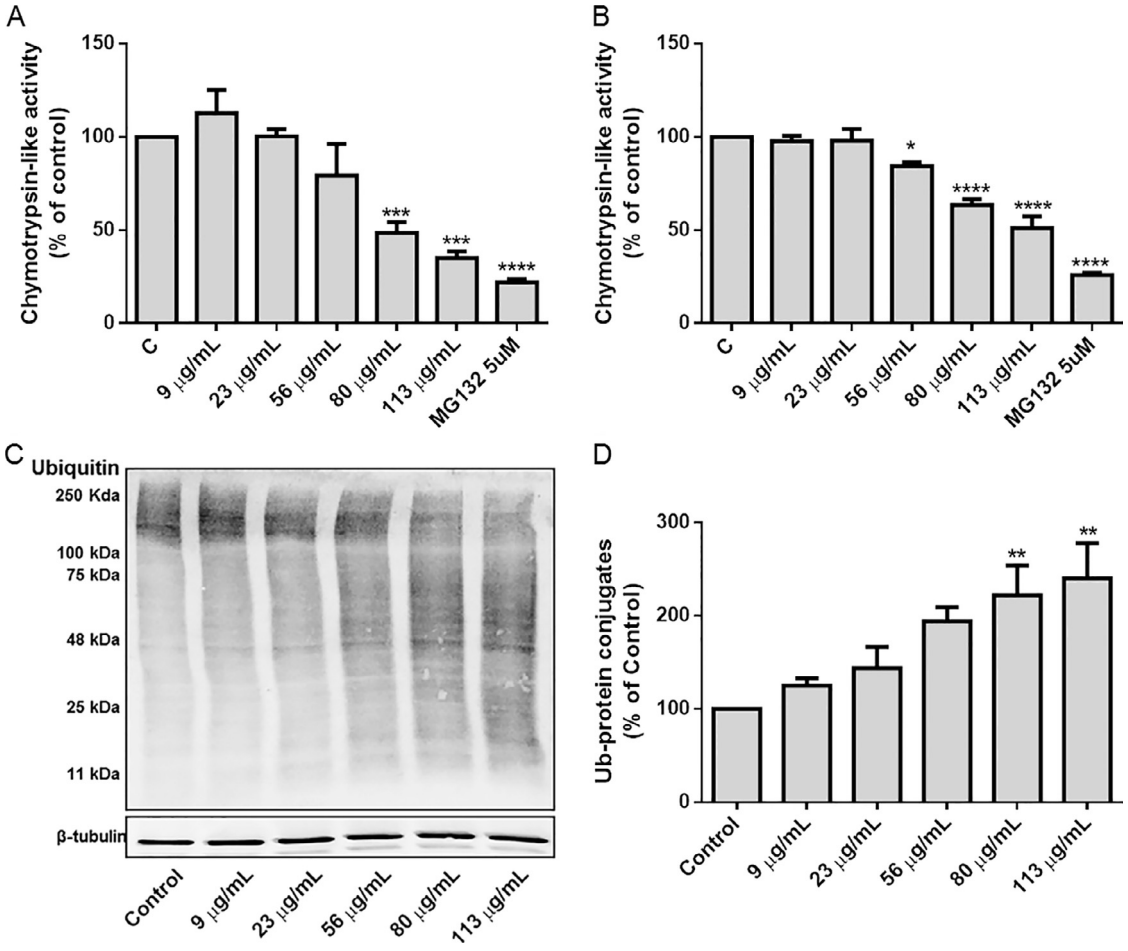

Figure 4 Effect of EEF on ubiquitin-proteasome system. Chymotrypsin-like activity of the 26S proteasome of cells treated with the EEF for 6 (A) and 24 h (B). Data are presented as mean ± SEM of, at least, 3 independent experiments and are expressed as percentage of control; Ubiquitinated proteins after incubation with EEF for 24 h were evaluated by western blot using an antibody against ubiquitin (P4D1). A representative immunoblot (C) and densitometric quantification of the whole lanes are presented (D). Data are presented as mean ± SEM of 4 independent experiments and are expressed as percentage of control ($^{*}p < 0.05$, $^{**}p < 0.01$, $^{***}p < 0.001$, $^{****}p < 0.0001$ when compared to control).

proteins was disclosed, suggesting an impairment of proteasome degradation (Fig. 4C and D), thus corroborating the previous results.

To evaluate whether EEF affects macroautophagy, we evaluated the levels of LC3-II after 6 h of treatment. The conjugation of LC3-I with phosphatidylethanolamine in the autophagic membranes leads to the formation of LC3-II, which is usually used as a measure of autophagosomes number and, at a certain point, constitutes a reliable marker of autophagic activity. However, besides the increase in autophagosomes formation, the increased amounts of LC3-II may also reflect the blockage of autophagosomes fusion with the lysosome (Klionsky et al., 2012), thus leading to an accumulation of these structures. Our data clearly demonstrate that EEF increased the expression of LC3-II in a dose-dependent way (Fig. 5) but, to further clarify the molecular mechanism behind autophagy modulation by EEF, we used chloroquine to measure the autophagic flux. Chloroquine is an inhibitor of autophagy that raises the lysosomal pH leading to the blockage of the fusion between autophagosomes and lysosomes and to the inhibition of lysosomal enzymes, thus decreasing protein degradation (Klionsky et al., 2012). As expected, cells treated with chloroquine elicited an accumulation of LC3-II. If the EEF was able to increase basal autophagy, cells co-incubated with chloroquine should present higher levels of LC3-II than cells treated with chloroquine alone. However, data show that the levels of LC3-II of cells treated with chloroquine or co-treated with EEF were similar (Fig. 5), suggesting that the effect of EEF on autophagy relies on the inhibition of autophagosomes degradation. Still, the mechanism underlying such effects needs further clarification, in order to understand how EEF impairs the autophagic clearance.

Recent studies demonstrated that polyphenols have a dual effect on autophagy, acting as either activators or inhibitors and it is widely accepted that an up-regulation of autophagy is beneficial in preventing aging and age-related diseases (Pallauf and Rimbach, 2013). However, given the dependence

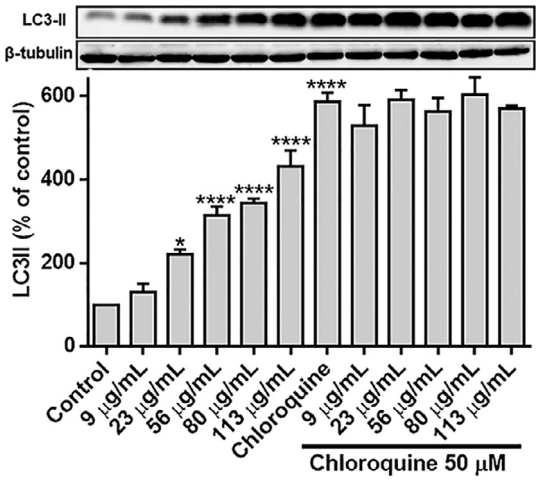

Figure 5 Effect of EEF on autophagy. Cells were treated with EEF alone or co-treated with chloroquine. A representative immunoblot is shown above the graph. Data are presented as mean ± SEM of, at least, 3 independent experiments and are expressed as percentage of control ($^{*}p < 0.01$, $^{****}p < 0.0001$ when compared to control).

of tumor cells on autophagy for their growth, the activation of this proteolytic pathway can promote the survival of cancer cells (Degenhardt et al., 2006). Accordingly, the inhibition of autophagy or the combination of autophagy inhibitors with anticancer agents has been proposed as a therapeutic strategy in cancer therapy (Amaravadi, 2009).

Regarding ellagitannins, there is very few information about the potential of these compounds to modulate the clearance mechanisms of the cells. To the best of our knowledge ellagitannins have not been reported as proteasome inhibitors, although their precursor, pentagalloylglucose, demonstrated anticancer effects through proteasome inhibition (Kuo et al., 2009) and ellagic acid was shown to inhibit 26S proteasome activity (Chang et al., 2013). Additionally, ellagic acid inhibited autophagy in ovarian cancer cells (Chung et al., 2013), while the ellagitannin punicalagin was able to induce autophagy in human glioma cells (Wang et al., 2013).

3.6. Identification of differentially expressed proteins in EEF-treated HepG2 cells

To further unveil other molecular targets of EEF, we evaluated changes induced by EEF in the proteome of HepG2 cells. For this purpose, we performed a comparative proteomics study using iTRAQ in cells incubated in the presence or absence of EEF (113 μg/mL for 24 h). Overall, this approach allowed the identification of 914 proteins, being 133 differentially expressed in EEF-treated cells (Fig. 6) (Supplementary Table 1). Looking at the biological processes and according to PANTHER classification system, those proteins are involved in metabolic pathways (39.5%), in cellular (18.4%) and developmental (7.9%) processes and also in cellular component organization or biogenesis (12.3%) (Fig. 7A).

A protein interaction network was generated with Cytoscape (ClueGO plugin), allowing the identification of proteins and biological processes which are either up- or down-regulated by EEF (Fig. 7B). The major clusters of interacting proteins are related to the regulation of translational elongation, *de novo* post-translational protein folding and several metabolic processes, as NADPH regeneration and glycolysis. It was also observed a down-regulation of several proteasome subunits, namely proteasome subunits alpha type-1 and -4, beta type -4 and 26S protease regulatory subunit 4, which are implicated in the regulation of cellular amine metabolic process, thus corroborating the inhibition of proteasome function, previously detected (Fig. 7B). The most significant cluster – cell metabolism, mainly covers the protein, nuclease-containing compound, carbohydrate and lipid metabolic processes. It is well established that cancer cells have altered metabolism, enabling its rapid proliferation and continuous growth (DeBerardinis et al., 2008). Hence, drugs that perturb cancer cell metabolism may open a perspective in cancer treatment.

Two of the most differently expressed proteins (FAS and IGFBP1) were chosen to validate the iTRAQ experiment by western blot. Besides the concentration used in proteomic experiments, lower concentrations were also tested in order to check whether the effects are dose-dependent. The results confirmed that EEF decreased FAS (Fig. 8A) and increased IGFBP1 (Fig. 8B), being those effects dependent on EEF concentration. IGFBPs interact with insulin-growth factors (IGF) I-II limiting their bioavailability. Since increased levels of insu-

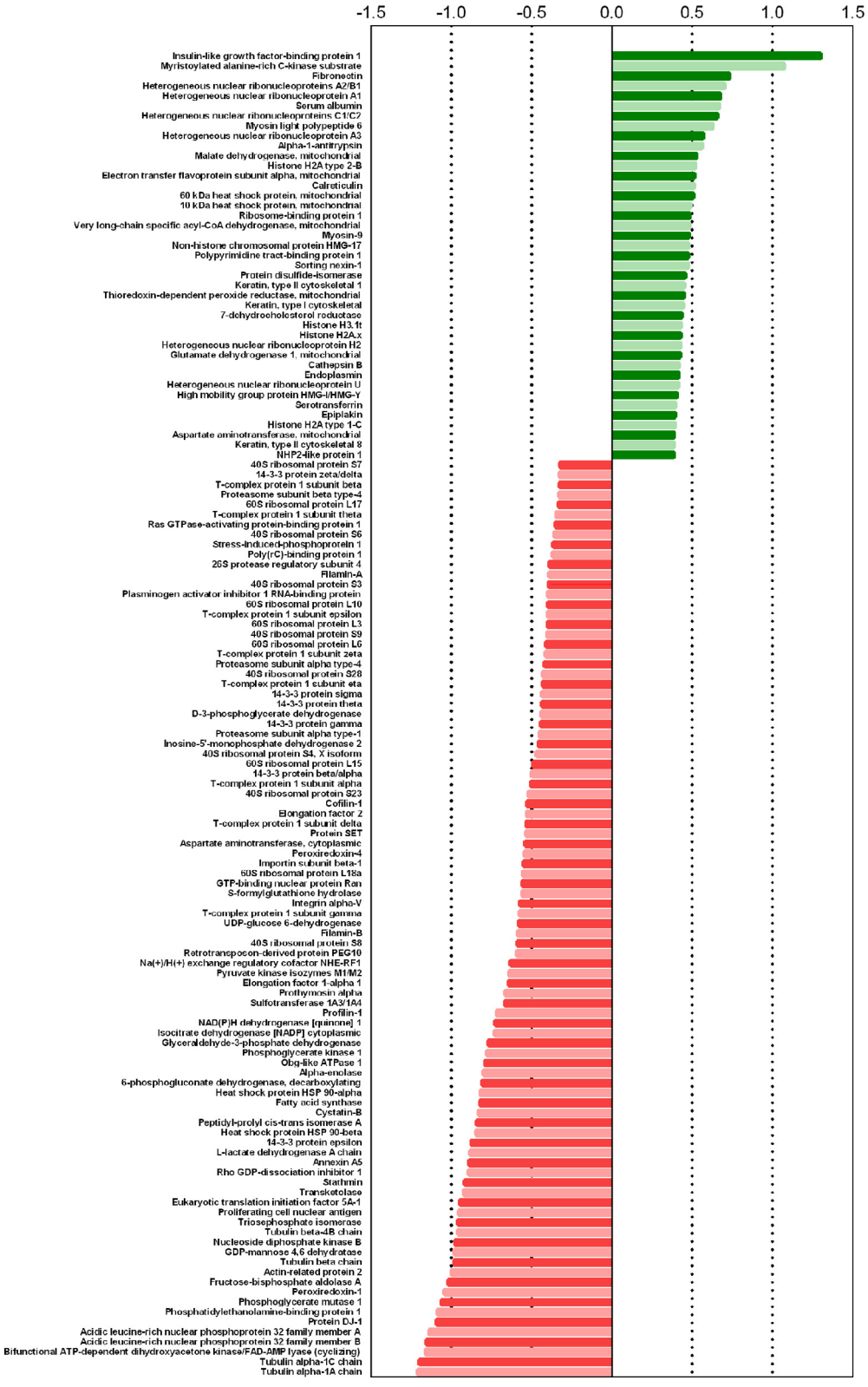

Figure 6 Log ratio comparison of the relative intensity for the significantly regulated proteins (EEF/Control).

lin and IGF have been linked to cancer progression (Yu, 2000), *F. vesca* leaves and particularly its EEF may be an important source of molecules able to disturb cancer cells metabolism and therefore represent an attractive therapeutic strategy for cancer. Increased fatty acid biosynthesis is also characteristic of cancer cells. FAS is a key enzyme for *de novo* fatty acid synthesis, catalyzing the conversion of acetyl-CoA and malonyl-CoA to palmitic acid. It was reported that enhanced FAS

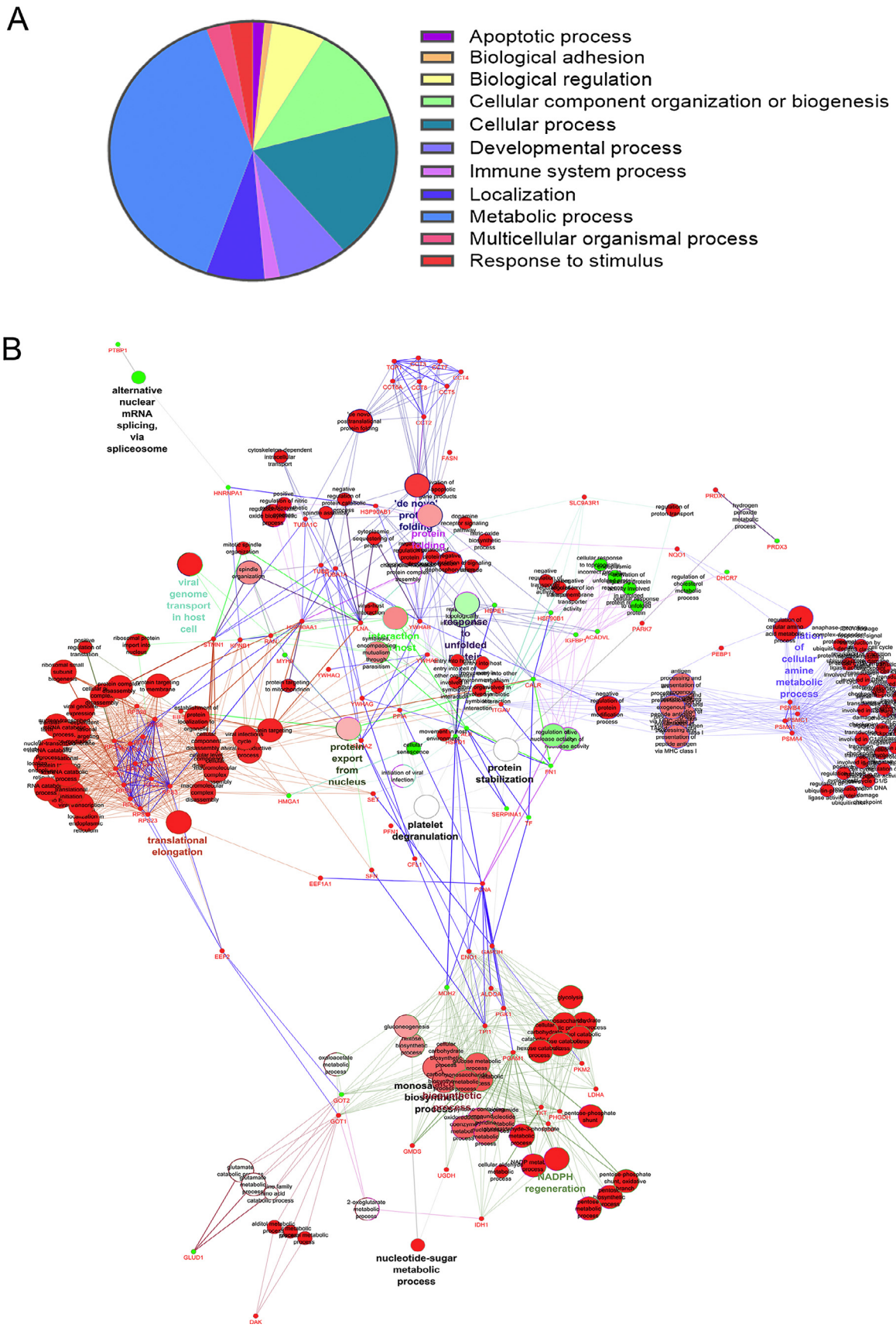

Figure 7 Effect of EEF on HepG2 proteome. (A) Distribution of differentially regulated proteins according to biological processes based on gene ontology annotation, after cells treatment with EEF. (B) Protein–protein interaction network generated with Cytoscape. Green nodes represent upregulated proteins while red nodes demonstrate downregulated proteins after 24 h of treatment with EEF.

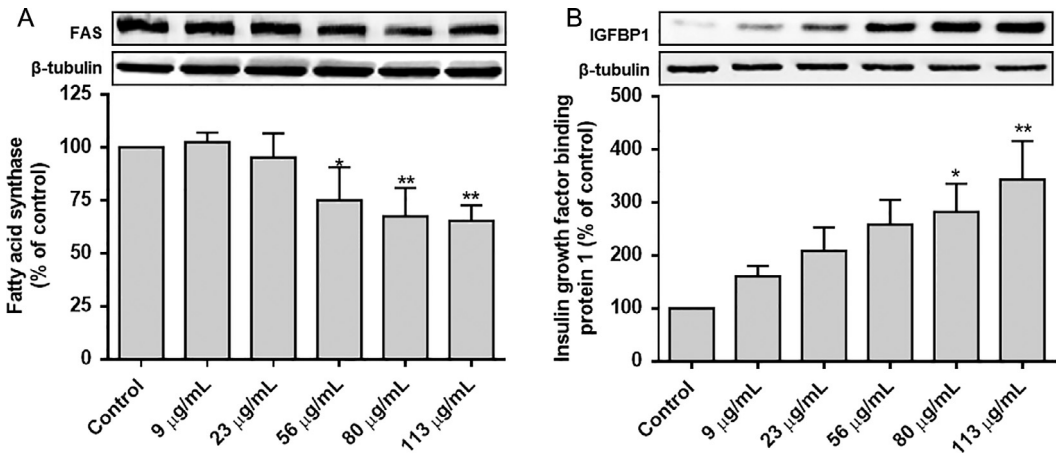

Figure 8 Effect of EEF on FAS and IGFBP1 protein levels. HepG2 cells were incubated with different concentrations of EEF fraction for 24 h and FAS (A) and IGFBP1 (B) protein levels were evaluated by western blot. Data are presented as mean ± SEM of, at least, 3 independent experiments and are expressed as percentage of control ($^{*}p < 0.05$, $^{**}p < 0.01$ when compared to control). Representative immunoblots are presented above the graphs.

expression and activity confer both growth and survival advantages in human tumors, including the hepatocellular carcinoma (Hao et al., 2014), being considered a metabolic oncogene. Moreover, several FAS inhibitors had shown antitumor activity, such as cerulenin (Pizer et al., 1996), the plant derived polyphenol curcumin (Fan et al., 2014) and epigallocatechin gallate (Brusselmans et al., 2003). In this work, we showed that EEF decreases FAS protein expression in a hepatocellular carcinoma cell line. Accordingly, Liu et al. (2009) reported that several ellagitannins were strong inhibitors of FAS activity. Taken together, ellagitannins might be potential anticancer molecules through the inhibition of FAS expression and activity.

4. Conclusion

The potential of polyphenols for cancer therapeutics has gained increased attention in the last years. Particularly, ellagitannins have been indicated as antiproliferative, antiangiogenic and pro-apoptotic compounds. In this study the phenolic characterization of an ellagitannin-enriched fraction from *F. vesca* leaves was performed. This fraction was more active than the crude extract in inhibiting HepG2 cell viability. Additionally, EEF also decreased cell proliferation, and induced the cell cycle arrest in G2/M. Our previous results strongly suggested that autophagy was modulated by the crude extract of *F. vesca* leaves. Herein, we demonstrated that EEF impairs autophagic flux, possibly leading to the cytoplasmic accumulation of autophagosomes that are not efficiently degraded. Along with the inhibition of autophagy, EEF also promoted the accumulation of ubiquitinated proteins, inhibited chymotrypsin-like activity of 26S proteasome and decreased the expression of several proteasome subunits, indicating an impairment of UPS degradation.

Furthermore, the proteomic analysis allowed the identification of differentially expressed proteins from several functional clusters, primarily affecting metabolic processes.

Overall, several cellular and molecular targets of EEF, and most probably of ellagitannins, were unveiled, suggesting that these compounds could be potential therapeutic agents against hepatocellular carcinoma. However, future studies should be considered in order to dissect the effect of EEF isolated compounds and also to investigate the synergism between ellagitannins and conventional chemotherapeutic agents.

Conflict of interest

No conflict to disclose.

Acknowledgments

We acknowledge FEDER/COMPETE (FCOMP-01-0124-FEDER-011096), Fundação para a Ciência e a Tecnologia – Portugal, European Union and QREN for funding the projects PTDC/SAU-FCF/105429/2008, PEst-C/SAU/LA0001/2013-2014, PEst-C/QUI/UI0062/2013, the Ph.D. fellowship SFRH/BD/72918/2010 and the QOPNA research unit (project PEst-C/QUI/UI0062/2013; FCOMP-01-0124-FEDER-037296). We also thank the Portuguese National Mass Spectrometry Network (RNEM, REDE/1504/REM/2005) for MS analyses obtained in Nodes CEF/Universidade de Coimbra and Universidade de Aveiro.

Appendix A. Supplementary material

Supplementary data associated with this article can be found, in the online version, at http://dx.doi.org/10.1016/j.arabjc.2015.11.014.

References

Aaby, K., Ekeberg, D., Skrede, G., 2007. Characterization of phenolic compounds in strawberry (Fragaria x ananassa) fruits by different HPLC detectors and contribution of individual compounds to total antioxidant capacity. J. Agric. Food Chem. 55, 4395–4406. http://dx.doi.org/10.1021/jf0702592.

Aguilera-Carbo, A., Augur, C., Prado-Barragan, L.A., Favela-Torres, E., Aguilar, C.N., 2008. Microbial production of ellagic acid and biodegradation of ellagitannins. Appl. Microbiol. Biotechnol. 78, 189–199. http://dx.doi.org/10.1007/s00253-007-1276-2.

Amaravadi, R., 2009. Autophagy can contribute to cell death when combining targeted therapy. Cancer Biol. Ther. 8, 130–133.

Arapitsas, P., 2012. Hydrolyzable tannin analysis in food. Food Chem. 135, 1708–1717. http://dx.doi.org/10.1016/j.foodchem.2012.05.096.

Ascacio-Valdes, J.A., Buenrostro-Figueroa, J.J., Aguilera-Carbo, A., Prado-Barragan, A., Rodriguez-Herrera, R., Aguilar, C.N., 2011. Ellagitannins: Biosynthesis, biodegradation and biological properties. J. Med. Plants Res. 5, 4696–4703.

Auzanneau, C., Montaudon, D., Jacquet, R., Puyo, S., Pouységu, L., Deffieux, D., Elkaoukabi-Chaibi, A., De Giorgi, F., Ichas, F., Quideau, S., Pourquier, P., 2012. The polyphenolic ellagitannin vescalagin acts as a preferential catalytic inhibitor of the α isoform of human DNA topoisomerase II. Mol. Pharmacol. 82, 134–141. http://dx.doi.org/10.1124/mol.111.077537.

Brusselmans, K., De Schrijver, E., Heyns, W., Verhoeven, G., Swinnen, J.V., 2003. Epigallocatechin-3-gallate is a potent natural inhibitor of fatty acid synthase in intact cells and selectively induces apoptosis in prostate cancer cells. Int. J. Cancer 106, 856–862. http://dx.doi.org/10.1002/ijc.11317.

Buricova, L., Andjelkovic, M., Cermakova, A., Reblova, Z., Jurcek, O., Kolehmainen, E., Verhe, R., Kvasnicka, F., 2011. Antioxidant capacities and antioxidants of strawberry, blackberry and raspberry leaves. Czech J. Food Sci. 29, 181–189.

Camejo-Rodrigues, J., Ascensão, L., Bonet, M.A., Vallès, J., 2003. An ethnobotanical study of medicinal and aromatic plants in the Natural Park of "Serra de São Mamede" (Portugal). J. Ethnopharmacol. 89, 199–209. http://dx.doi.org/10.1016/S0378-8741(03)00270-8.

Center, M.M., Jemal, A., 2011. International trends in liver cancer incidence rates. Cancer Epidemiol. Biomarkers Prev. 20, 2362–2368. http://dx.doi.org/10.1158/1055-9965.EPI-11-0643.

Chang, T.-L., Lin, S.-W., Wu, S., Hong, C.-M., 2013. Regulation of ubiquitin and 26S proteasome mediated by phenolic compounds during oxidative stress. J. Nutr. Biochem. 24, 1970–1981. http://dx.doi.org/10.1016/j.jnutbio.2013.07.001.

Cho, H., Jung, H., Lee, H., Yi, H.C., Kwak, H.-K., Hwang, K.T., 2015. Chemopreventive activity of ellagitannins and their derivatives from black raspberry seeds on HT-29 colon cancer cells. Food Funct. 6, 1675–1683. http://dx.doi.org/10.1039/c5fo00274e.

Chung, Y.-C., Lu, L.-C., Tsai, M.-H., Chen, Y.-J., Chen, Y.-Y., Yao, S.-P., Hsu, C.-P., 2013. The inhibitory effect of ellagic acid on cell growth of ovarian carcinoma cells. Evidence-Based Complement. Altern. Med. 2013, 306705. http://dx.doi.org/10.1155/2013/306705.

Daniel, E.M., Ratnayake, S., Kinstle, T., Stoner, G.D., 1991. The Effects of pH and Rat Intestinal Contents on the Liberation of Ellagic Acid from Purified and Crude Ellagitannins. J. Nat. Prod. 54, 946–952. http://dx.doi.org/10.1021/np50076a004.

DeBerardinis, R.J., Lum, J.J., Hatzivassiliou, G., Thompson, C.B., 2008. The biology of cancer: metabolic reprogramming fuels cell growth and proliferation. Cell Metab. 7, 11–20. http://dx.doi.org/10.1016/j.cmet.2007.10.002.

Degenhardt, K., Mathew, R., Beaudoin, B., Bray, K., Anderson, D., Chen, G., Mukherjee, C., Shi, Y., Gélinas, C., Fan, Y., Nelson, D. A., Jin, S., White, E., 2006. Autophagy promotes tumor cell survival and restricts necrosis, inflammation, and tumorigenesis. Cancer Cell 10, 51–64. http://dx.doi.org/10.1016/j.ccr.2006.06.001.

Driscoll, J.J., Chowdhury, R.De., 2012. Molecular crosstalk between the proteasome, aggresomes and autophagy: translational potential and clinical implications. Cancer Lett. 325, 147–154. http://dx.doi.org/10.1016/j.canlet.2012.06.016.

El-Serag, H.B., Rudolph, K.L., 2007. Hepatocellular carcinoma: epidemiology and molecular carcinogenesis. Gastroenterology 132, 2557–2576. http://dx.doi.org/10.1053/j.gastro.2007.04.061.

Fan, H., Tian, W., Ma, X., 2014. Curcumin induces apoptosis of HepG2 cells via inhibiting fatty acid synthase. Target. Oncol. 9, 279–286. http://dx.doi.org/10.1007/s11523-013-0286-5.

Feitelson, M.A., Arzumanyan, A., Kulathinal, R.J., Blain, S.W., Holcombe, R.F., Mahajna, J., Marino, M., Martinez-Chantar, M. L., Nawroth, R., Sanchez-Garcia, I., Sharma, D., Saxena, N.K., Singh, N., Vlachostergios, P.J., Guo, S., Honoki, K., Fujii, H., Georgakilas, A.G., Amedei, A., Niccolai, E., Amin, A., Ashraf, S. S., Boosani, C.S., Guha, G., Ciriolo, M.R., Aquilano, K., Chen, S., Mohammed, Azmi, A.S., Bhakta, D., Halicka, D., Nowsheen, S., 2015. Sustained proliferation in cancer: Mechanisms and novel therapeutic targets. Semin. Cancer Biol. 1–30. http://dx.doi.org/10.1016/j.semcancer.2015.02.006.

Festjens, N., Vanden Berghe, T., Vandenabeele, P., 2006. Necrosis, a well-orchestrated form of cell demise: signalling cascades, important mediators and concomitant immune response. Biochim. Biophys. Acta 1757, 1371–1387. http://dx.doi.org/10.1016/j.bbabio.2006.06.014.

Fresco, P., Borges, F., Marques, M.P.M., Diniz, C., 2010. The anticancer properties of dietary polyphenols and its relation with apoptosis. Curr. Pharm. Des. 16, 114–134. http://dx.doi.org/10.2174/138161210789941856.

Gasperotti, M., Masuero, D., Guella, G., Palmieri, L., Martinatti, P., Pojer, E., Mattivi, F., Vrhovsek, U., 2013. Evolution of ellagitannin content and profile during fruit ripening in Fragaria spp. J. Agric. Food Chem. 61, 8597–8607. http://dx.doi.org/10.1021/jf402706h.

Giampieri, F., Tulipani, S., Alvarez-Suarez, J.M., Quiles, J.L., Mezzetti, B., Battino, M., 2012. The strawberry: Composition, nutritional quality, and impact on human health. Nutrition 28, 9–19. http://dx.doi.org/10.1016/j.nut.2011.08.009.

Giovannini, C., Masella, R., 2012. Role of polyphenols in cell death control. Nutr. Neurosci. 15, 134–149. http://dx.doi.org/10.1179/1476830512Y.0000000006.

Gođevac, D., Tešević, V., Vajs, V., Milosavljević, S., Stanković, M., 2011. Blackberry seed extracts and isolated polyphenolic compounds showing protective effect on human lymphocytes DNA. J. Food Sci. 76, C1039–C1043. http://dx.doi.org/10.1111/j.1750-3841.2011.02305.x.

Hanhineva, K., Rogachev, I., Kokko, H., Mintz-Oron, S., Venger, I., Kärenlampi, S., Aharoni, A., 2008. Non-targeted analysis of spatial metabolite composition in strawberry (Fragaria×ananassa) flowers. Phytochemistry 69, 2463–2481. http://dx.doi.org/10.1016/j.phytochem.2008.07.009.

Hao, Q., Li, T., Zhang, X., Gao, P., Qiao, P., Li, S., Geng, Z., 2014. Expression and roles of fatty acid synthase in hepatocellular carcinoma. Oncol. Rep. 32, 2471–2476. http://dx.doi.org/10.3892/or.2014.3484.

Ivanov, I., Petkova, N., Denev, P., Pavlov, A., 2015. Polyphenols content and antioxidant activities in infusion and decoction extracts obtained from *Fragaria vesca* L. leaves. Sci. Bull. Ser. F. Biotechnol. 19, 145–148.

Kampa, M., Nifli, A.-P., Notas, G., Castanas, E., 2007. Polyphenols and cancer cell growth. Rev. Physiol. Biochem. Pharmacol. 159, 79–113. http://dx.doi.org/10.1007/112_2006_0702.

Kasimsetty, S.G., Bialonska, D., Reddy, M.K., Ma, G., Khan, S.I., Ferreira, D., 2010. Colon cancer chemopreventive activities of pomegranate ellagitannins and urolithins. J. Agric. Food Chem. 58, 2180–2187. http://dx.doi.org/10.1021/jf903762h.

Klionsky, D.J. et al, 2012. Guidelines for the use and interpretation of assays for monitoring autophagy. Autophagy 8, 445–544.

Kool, M.M., Comeskey, D.J., Cooney, J.M., McGhie, T.K., 2010. Structural identification of the main ellagitannins of a boysenberry (Rubus loganbaccus×baileyanus Britt.) extract by LC–ESI-MS/MS. MALDI-TOF-MS and NMR spectroscopy. Food Chem. 119, 1535–1543. http://dx.doi.org/10.1016/j.foodchem.2009.09.039.

Kuo, P.-L., Hsu, Y.-L., Lin, T.-C., Chang, J.-K., Lin, C.-C., 2005a. Induction of cell cycle arrest and apoptosis in human non-small cell lung cancer A549 cells by casuarinin from the bark of *Terminalia arjuna* Linn. Anticancer. Drugs 16, 409–415.

Kuo, P.-L., Hsu, Y.-L., Lin, T.-C., Lin, L.-T., Chang, J.-K., Lin, C.-C., 2005b. Casuarinin from the Bark of *Terminalia arjuna* induces apoptosis and cell cycle arrest in human breast adenocarcinoma MCF-7 cells. Planta Med. 71, 237–243. http://dx.doi.org/10.1055/s-2005-837823.

Kuo, P.-T., Lin, T.-P., Liu, L.-C., Huang, C.-H., Lin, J.-K., Kao, J.-Y., Way, T.-D., 2009. Penta-O-galloyl-β-d-glucose suppresses

prostate cancer bone metastasis by transcriptionally repressing EGF-induced MMP-9 expression. J. Agric. Food Chem. 57, 3331–3339. http://dx.doi.org/10.1021/jf803725h.

Lee, J.H., Talcott, S.T., 2002. Ellagic acid and ellagitannins affect on sedimentation in muscadine juice and wine. J. Agric. Food Chem. 50, 3971–3976. http://dx.doi.org/10.1021/jf011587j.

Li, J., Wang, S., Yin, J., Pan, L., 2013. Geraniin induces apoptotic cell death in human lung adenocarcinoma A549 cells in vitro and in vivo. Can. J. Physiol. Pharmacol. 91, 1016–1024. http://dx.doi.org/10.1139/cjpp-2013-0140.

Liberal, J., Francisco, V., Costa, G., Figueirinha, A., Amaral, M.T., Marques, C., Girão, H., Lopes, M.C., Cruz, M.T., Batista, M.T., 2014. Bioactivity of *Fragaria vesca* leaves through inflammation, proteasome and autophagy modulation. J. Ethnopharmacol. 158PA, 113–122. http://dx.doi.org/10.1016/j.jep.2014.09.043.

Lin, S., Hoffmann, K., Schemmer, P., 2012. Treatment of hepatocellular carcinoma: a systematic review. Liver cancer 1, 144–158. http://dx.doi.org/10.1159/000343828.

Liu, H., Li, J., Zhao, W., Bao, L., Song, X., Xia, Y., Wang, X., Zhang, C., Wang, X., Yao, X., Li, M., 2009. Fatty Acid Synthase Inhibitors from Geum japonicum Thunb. var. chinense. Chem. Biodivers. 6, 402–410. http://dx.doi.org/10.1002/cbdv.200700462.

Mullen, W., Yokota, T., Lean, M.E.J., Crozier, A., 2003. Analysis of ellagitannins and conjugates of ellagic acid and quercetin in raspberry fruits by LC–MSn. Phytochemistry 64, 617–624. http://dx.doi.org/10.1016/S0031-9422(03)00281-4.

Neves, J.M., Matos, C., Moutinho, C., Queiroz, G., Gomes, L.R., 2009. Ethnopharmacological notes about ancient uses of medicinal plants in Trás-os-Montes (northern of Portugal). J. Ethnopharmacol. 124, 270–283. http://dx.doi.org/10.1016/j.jep.2009.04.041.

O'Brien, J., Wilson, I., Orton, T., Pognan, F., 2000. Investigation of the Alamar Blue (resazurin) fluorescent dye for the assessment of mammalian cell cytotoxicity. Eur. J. Biochem. 267, 5421–5426. http://dx.doi.org/10.1046/j.1432-1327.2000.01606.x.

Okuda, T., Yoshida, T., Hatano, T., 1993. Classification of oligomeric hydrolysable tannins and specificity of their occurrence in plants. Phytochemistry 32, 507–521. http://dx.doi.org/10.1016/S0031-9422(00)95129-X.

Pallauf, K., Rimbach, G., 2013. Autophagy, polyphenols and healthy ageing. Ageing Res. Rev. 12, 237–252. http://dx.doi.org/10.1016/j.arr.2012.03.008.

Pizer, E.S., Jackisch, C., Wood, F.D., Pasternack, G.R., Davidson, N.E., Kuhajda, F.P., 1996. Inhibition of fatty acid synthesis induces programmed cell death in human breast cancer cells. Cancer Res. 56, 2745–2747.

Proskuryakov, S., Gabai, V., 2010. Mechanisms of tumor cell necrosis. Curr. Pharm. Des. 16, 56–68. http://dx.doi.org/10.2174/138161210789941793.

Quideau, S., 2009. Chemistry and Biology of Ellagitannins. World Scientific. http://dx.doi.org/10.1142/6795.

Ramos, S., 2008. Cancer chemoprevention and chemotherapy: dietary polyphenols and signalling pathways. Mol. Nutr. Food Res. 52, 507–526. http://dx.doi.org/10.1002/mnfr.200700326.

Ross, H.A., McDougall, G.J., Stewart, D., 2007. Antiproliferative activity is predominantly associated with ellagitannins in raspberry extracts. Phytochemistry 68, 218–228. http://dx.doi.org/10.1016/j.phytochem.2006.10.014.

Sartippour, M.R., Seeram, N.P., Rao, J.Y., Moro, A., Harris, D.M., Henning, S.M., Firouzi, A., Rettig, M.B., Aronson, W.J., Pantuck, A.J., Heber, D., 2008. Ellagitannin-rich pomegranate extract inhibits angiogenesis in prostate cancer in vitro and in vivo. Int. J. Oncol. 32, 475–480.

Simirgiotis, M.J., Schmeda-Hirschmann, G., 2010. Determination of phenolic composition and antioxidant activity in fruits, rhizomes and leaves of the white strawberry (Fragaria chiloensis spp. chiloensis form chiloensis) using HPLC-DAD–ESI-MS and free radical quenching techniques. J. Food Compos. Anal. 23, 545–553. http://dx.doi.org/10.1016/j.jfca.2009.08.020.

Vassallo, A., Vaccaro, M.C., De Tommasi, N., Dal Piaz, F., Leone, A., 2013. Identification of the plant compound Geraniin as a Novel Hsp90 inhibitor. PLoS One 8, e74266. http://dx.doi.org/10.1371/journal.pone.0074266.

Vilchez, D., Saez, I., Dillin, A., 2014. The role of protein clearance mechanisms in organismal ageing and age-related diseases. Nat. Commun. 5, 5659. http://dx.doi.org/10.1038/ncomms6659.

Vitorino, R., Guedes, S., Manadas, B., Ferreira, R., Amado, F., 2012. Toward a standardized saliva proteome analysis methodology. J. Proteomics 75, 5140–5165. http://dx.doi.org/10.1016/j.jprot.2012.05.045.

Vrhovsek, U., Guella, G., Gasperotti, M., Pojer, E., Zancato, M., Mattivi, F., 2012. Clarifying the identity of the main ellagitannin in the fruit of the strawberry, *Fragaria vesca* and *Fragaria ananassa* Duch. J. Agric. Food Chem. 60, 2507–2516. http://dx.doi.org/10.1021/jf2052256.

Wang, B., Jin, Z., 2011. Agrimoniin induced SGC7901 cell apoptosis associated mitochondrial transmembrane potential and intracellular calcium concentration. J. Med. Plants Res. 5, 3512–3519.

Wang, S., Huang, M., Li, J., Lai, F., Lee, H., Hsu, Y., 2013. Punicalagin induces apoptotic and autophagic cell death in human U87MG glioma cells. Acta Pharmacol. Sin. 34, 1411–1419. http://dx.doi.org/10.1038/aps.2013.98.

Wang, Y., Ma, J., Chow, S.C., Li, C.H., Xiao, Z., Feng, R., Fu, J., Chen, Y., 2014. A potential antitumor ellagitannin, davidiin, inhibited hepatocellular tumor growth by targeting EZH2. Tumor Biol. 35, 205–212. http://dx.doi.org/10.1007/s13277-013-1025-3.

Yu, H., 2000. Role of the insulin-like growth factor family in cancer development and progression. J. Natl. Cancer Inst. 92, 1472–1489. http://dx.doi.org/10.1093/jnci/92.18.1472.